JOURNAL OF COMPUTATIONAL PHYSICS 105, 279–289 (1993)

Automatic Feynman Graph Generation

P. NOGUEIRA

CFMC - INIC, Av. Prof. Gama Pinto 2, P-1699 Lisboa Codex, Portugal

Received August 6, 1991

A general method is devised for the automatic generation of Feynman diagrams in gauge (and other) field theories. The performance of an implemented computer program is also described, as well as a number of tests that rely on complementary enumeration techniques.

1. INTRODUCTION

In the world of high-energy physics, gauge field theories seem to play a very special role. They are thought to describe basic interactions among elementary particles. Their appeal has increased since it was verified that electroweak interactions appear to be described by a *perturbative* gauge field theory. However, the complexity of a theory like the standard model, due both to the large number of elementary fields and to a variety of interactions, makes unpractical almost every calculation beyond tree level since the number of diagrams involved becomes very large. This problem will be even more acute if a supersymmetric field theory becomes necessary. In order to enlarge the class of feasible calculations, critical in precise measurements at high energy, automatic methods must be developed. Some recent progress has been done by Boos *et al.* [1], who have designed a computer program to compute tree level processes characteristics in gauge theories.

The subject of automatic generation of Feynman diagrams has been approached by several authors in the last two decades [2–5]. However, none of the available computer programs is entirely satisfactory. Most of them are simply restricted to a particular interaction (QED). Until recently, the most interesting program was FRENEY [3], which accepts a mixture of interactions and still performs the elimination of equivalent diagrams. Nonetheless, obtaining all diagrams for a given process is not completely automatic: several runs are needed, depending on the number of possibilities of combining interactions (and this must be done by hand).

After the completion of this work I have learned about a recent paper by Küblbeck *et al.* [6] that addresses the same problem. However, the following should be noted: their algorithm depends mainly on two techniques (recursive generation of diagrams and comparison of stored diagrams) that were deliberately avoided in the present paper; typical execution times are large and so only a restricted class of physical processes may be approached by their computer program; the enumeration issue is dealt with in a far less complete way.

This paper is organized as follows: Section 2 describes an algorithm for automatic graph generation in any perturbative field theory, except for the elimination of equivalent graphs that is described in Section 3. In Section 4 a number of tests that may be applied to any such computer program are presented. A computer program has been developed to check for the feasibility of this approach; a few of its characteristics and an analysis of its performance are given in Section 5. Appendix A contains most enumeration results while Appendix B is devoted to special topics: one-particle irreducible diagrams and diagrams without tadpoles.

2. THE METHOD

Although the present approach relies directly on graph theory not all the graph theory concepts used throughout this paper will be defined in detail; see, for instance, the book by Harray [7] for complementary information.

The basic structures here considered are the so-called pseudographs: these consist of a set of nodes (vertices) that may be joined by edges (lines); multiple edges and *loops* (edges that join a node to itself) are possible. To avoid confusion with the field theory terminology, the word *loop* will be italicized whenever used in the context of graph theory. What physicists call the number of loops is known to mathematicians as the *cyclomatic number*. Define a *bond* as a set of all the edges adjacent to exactly the same nodes.

Every pseudograph may be represented by its adjacency matrix, in which a certain entry $a_{i,j}$ denotes the number of edges joining nodes i and j. The valency of a node (in the literature, the designation *valency* is often replaced by *degree*) is the number of lines adjacent to it (*loops* counting

0021-9991/93 $5.00

twice). If a pseudograph has exactly n_1 nodes of valency 1, n_2 nodes of valency 2,..., n_k nodes of valency k, one says it has (node valency) partition $(n_1, n_2, ..., n_k)$; since for our purposes n_2 will be always zero, it will be omitted in the following.

There is a direct equivalence between a pseudograph and the underlying topology of a Feynman diagram: an external particle may be associated with a node of valency 1 (or endnode) and an interaction vertex with a node of higher valency, usually 3 or 4.

A Feynman diagram is a more complex structure than a pseudograph: first, there may be distinct fields, and thus the need to assign different colours to its edges; second, some particles may be different from their antiparticles, forcing us to use directed edges to distinguish between the two "charge" flows; third, the external particles are considered as distinguishable so as to draw all diagrams, and thus all endnodes must be labelled. The word *colouring* will be used in a way that is not consistent with the usual terminology in graph theory; in this paper it will mean attaching (possibly directed) propagators to the pseudograph edges. In this combinatorial approach propagators are represented by ordered pairs of conjugated fields $(p, \bar{p})$; for fields that are not self-conjugate ($p \neq \bar{p}$) an orientation is automatically assigned to a propagator. In turn, interaction vertices may be represented by sets of fields $\{p_1, p_2, ..., p_n\}$ with $n \geqslant 3$; this defines the way propagators can meet at the nodes.

The algorithm strategy is divided into the following steps (except for the graph elimination part):

1. generation of the connected unlabelled pseudographs whose nodes have valencies allowed by the given field theory (1, 3, and 4 for a gauge field theory); the number of such nodes is determined by the number of external particles and the order of perturbation theory

2. generation of the connected pseudographs with all endnodes labelled (for each pseudograph obtained in step 1 one labels the endnodes in all possible ways)

3. colouring each labelled pseudograph obtained in step 2 in all ways compatible with the vertex rules; this means that one associates a (possibly directed) propagator to each edge such that at every node one obtains a possible interaction vertex. Note that at this point the entire graph is effectively labelled.

The generation of the connected pseudographs will not be described in detail. In general terms, it consists of constructing all adjacency matrices that have a given node partition. When representing a pseudograph by its adjacency matrix one is effectively labelling all nodes. So, for practical matters, a set of unlabelled (pseudo)graphs is in fact a set of labelled (pseudo)graphs no two of which have similar adjacency matrices (matrices that may be transformed into one another by permuting nodes). Care has to be taken in order not to generate similar matrices. An orderly type algorithm has been chosen so that no comparison with previously generated graphs is needed. Reference [8] describes a possible algorithm and contains a list of relevant papers; although this material is devoted to graphs it is a simple matter to extend it to the case of pseudographs.

3. SYMMETRY

In the method just described, nontrivial symmetries will inevitably lead to the generation of equivalent Feynman diagrams during the labelling and colouring procedures. However, it is desirable that one selects only a single diagram (the "representative" diagram) out of a class of equivalent diagrams. The elimination procedure that was adopted relies on the construction of the symmetry (automorphism) group of the underlying pseudograph. The following symmetry groups are used:

- $\Gamma_P(G)$, the point symmetry group of the pseudograph G, which consists of the node permutations for which the adjacency matrix is invariant
- $\Gamma_I(G)$, the subgroup of Γ_P that leaves the endnodes fixed
- $\Gamma_F(G)$, the subgroup of Γ_I for which a certain Feynman graph F is invariant; it is assumed that G is the graph topology of F.

Symmetries involving edge permutations are also possible, and each such symmetry may be obtained by a composition of the following operations:

- permutation of edges within each bond (if there are m edges this gives a *local* symmetry group S_m)
- permutation of bonds together with the induced permutation of nodes; it is important to note that for a connected pseudograph with n nodes, this group is isomorphic to Γ_P if $n > 2$ (this follows trivially from a result obtained by Sabidussi [9]).

A total order relation $\prec$ will be needed below (any properly defined relation $\prec$ will do). The nodes of a pseudograph, the edges within each bond, and the fields are assumed to be ordered according to $\prec$; n-tuples and higher dimensional structures can be ordered in the usual way: for example, given two n-tuples $(r_1, r_2, ..., r_k)$ and $(s_1, s_2, ..., s_k)$ one writes $\mathbf{r} \prec \mathbf{s}$ if there is an index j for which $r_j \prec s_j$ and $r_i = s_i$ for all $i < j$.

After a given pseudograph and its point symmetry group Γ_P have been obtained, the endnodes are given a label e_i, $i = 1, 2, ..., n_1$, to denote which external particle will be mapped to each such node. However, as some of these

possibilities might be equivalent, an elimination criterion is defined as follows: given a label $\mathbf{e}$ obtain, for all permutations $P \in \Gamma_P$, the permuted labels $\mathbf{e}_P$; a given labelling is dicarded if and only if $\mathbf{e}_P \prec \mathbf{e}$ for some P, that is, unless $\mathbf{e}$ is the "minimum label" (according to $\prec$).

At the last step one must decide whether to keep or reject a given Feynman graph. Two symmetry sources may then yield equivalent Feynman graphs: the first possibility is that there may be *loops* or multiple edges, and the other is that Γ_I might not be the identity group. The former case is overcome in the following way:

- if there are m edges joining nodes v_i and v_j, where $v_i \prec v_j$, then one demands (see Fig. 1) $p_1 \preccurlyeq p_2 \preccurlyeq \cdots \preccurlyeq p_m$
- if there are m *loops* at node v_k one requires (see Fig. 1) $p_i \preccurlyeq \bar{p}_i$ and $p_i \preccurlyeq p_{i+1}$ for all i.

The latter possibility is dealt with a variation of the method used before: build any structure $X(F)$, which may be one-dimensional, two-dimensional, ..., but capable of univocally defining a Feynman graph F. For example, this structure may consist of a list of the propagators attached to every edge, in a specified order. Under the action of any permutation $P \in \Gamma_I$, F transforms into an equivalent graph F_P, represented by $X(F_P)$. A given Feynman graph F is retained iff $X(F) \preccurlyeq X(F_P)$ for all $P \in \Gamma_I$.

The computation of the topological symmetry factor is also possible and quite straightforward in this scheme. This symmetry factor is always the reciprocal of an integer (call it the symmetry number of the Feynman diagram) that may be obtained by the combined multiplication of the following factors:

- for each set of m identical propagators within the same bond a *local factor* $m!$ unless the propagators are undirected *loops* (the factor is then $(2m)!!$)
- a single *global factor* $|\Gamma_F|$.

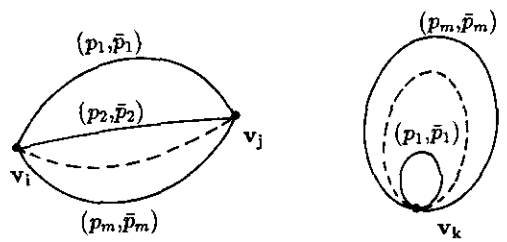

FIG. 1. Selection rules in the case of *loops* and multiple edges. The propagators are represented by ordered pairs of conjugated fields $(p, \bar{p})$; assume that the particle p_k moves from v_j to v_i (or equivalently, that $\bar{p}_k$ moves in the opposite direction). On the left, only the edge permutation symmetry must be broken. The presence of *loops* (right) requires extra conditions to break the *loop* reversal symmetry (that is, inverting the propagators).

The symmetry number is, clearly, the order of the residual line symmetry group if one includes *loop* reversal as an acceptable operation (for a Feynman diagram *loop* reversal may be defined as the inversion of the associated propagator).

4. TESTING

A completely general set of checks is clearly not possible. Nonetheless, you may find below a number of fairly stringent tests. Nearly all the calculations involved in this section were performed by different REDUCE [10] programs. Most of the results are given in Table I and in the Appendix.

In the first place, one should check whether all distinct graph topologies are indeed generated; to this purpose the number of connected pseudographs (all nodes unlabelled) has been computed (see Table I). The number of possibly disconnected unlabelled pseudographs with partition (n_1, n_3, n_4) is [11]

$$P^{n_1 n_3 n_4} = N\{Z(S_{n_1}[S_1] \times S_{n_3}[S_3] \times S_{n_4}[S_4]) * Z(S_l[S_2])\}, \tag{1}$$

where S_n is the symmetric group of degree n and $l = (n_1 + 3n_3 + 4n_4)/2$ is the number of edges. $Z(H)$ denotes the cycle-index of the permutation group H; the direct product and the composition of two groups H_1 and H_2 are denoted by $H_1 \times H_2$ and $H_1[H_2]$, respectively; $N\{Z(H_1) * Z(H_2)\}$ stands for the number of graphs obtained according to the superposition theorem [11].

If these pseudographs are required to be connected, their numbers $p^{n_1 n_3 n_4}$ may be computed using the relation between the total and the connected counting series for a certain type of graphs [12]. The results are given in Table I. The following truncation has been used:

$$\begin{aligned} n_1 &\leqslant 7 \\ n_3 + 2n_4 &\leqslant 9 \\ n_1 + n_3 + 2n_4 &\leqslant 12. \end{aligned} \tag{2}$$

These bounds were chosen in accordance with the input range for the computer program (see conditions (16) below).

It is also possible to compute such numbers when some (or all) classes of nodes are labelled; in the case of interest here, the coefficients of the counting series of all graphs are [11]

$$P_1^{n_1 n_3 n_4} = N\{Z(E_{n_1}[S_1] \times S_{n_3}[S_3] \times S_{n_4}[S_4]) * Z(S_l[S_2])\}, \tag{3}$$

TABLE I

Numbers of Various Kinds of Connected Graphs: Pseudographs (p), Pseudographs with Labelled Endnodes (p_1) and Digraphs of Type $\bar{d}_1$ (See Eqs. (11) and (12)) with Given Partition

(n_1, n_3, n_4)	p	p_1	$\bar{d}_1$	(n_1, n_3, n_4)	p	p_1	$\bar{d}_1$
(0, 0, 1)	1	1	1	(3, 3, 1)	36	117	1748
(0, 0, 2)	2	2	5	(3, 3, 2)	362	1318	60,294
(0, 0, 3)	4	4	23	(3, 3, 3)	3312	13,142	1,937,184
(0, 0, 4)	10	10	179	(3, 5, 0)	19	58	1836
(0, 2, 0)	2	2	3	(3, 5, 1)	427	1621	156,070
(0, 2, 1)	5	5	33	(3, 5, 2)	6897	28,471	8,950,140
(0, 2, 2)	22	22	425	(3, 7, 0)	147	535	107,060
(0, 2, 3)	88	88	6435	(3, 7, 1)	5229	21,968	14,398,448
(0, 4, 0)	5	5	40	(3, 9, 0)	1326	5427	7,335,800
(0, 4, 1)	30	30	1261	(4, 0, 0)	0	0	0
(0, 4, 2)	228	228	36,040	(4, 0, 1)	1	1	1
(0, 6, 0)	17	17	870	(4, 0, 2)	2	7	17
(0, 6, 1)	193	193	61,020	(4, 0, 3)	8	42	291
(0, 8, 0)	71	71	31,052	(4, 0, 4)	37	255	5293
(1, 1, 0)	1	1	1	(4, 2, 0)	1	3	6
(1, 1, 1)	3	3	9	(4, 2, 1)	8	53	280
(1, 1, 2)	10	10	83	(4, 2, 2)	73	598	9094
(1, 1, 3)	39	39	1023	(4, 2, 3)	575	5784	269828
(1, 1, 4)	174	174	14,941	(4, 4, 0)	6	39	444
(1, 3, 0)	3	3	16	(4, 4, 1)	114	1109	36,028
(1, 3, 1)	24	24	421	(4, 4, 2)	1698	19,223	1,927,682
(1, 3, 2)	172	172	10,055	(4, 6, 0)	50	465	31,992
(1, 3, 3)	1211	1211	244,378	(4, 6, 1)	1582	19,164	4,052,368
(1, 5, 0)	12	12	376	(4, 8, 0)	475	5625	2,490,264
(1, 5, 1)	193	193	22,922	(5, 1, 0)	0	0	0
(1, 5, 2)	2390	2390	1,016,836	(5, 1, 1)	1	10	20
(1, 7, 0)	67	67	14,116	(5, 1, 2)	8	145	760
(1, 7, 1)	1745	1745	1,490,054	(5, 1, 3)	59	1485	22,620
(1, 9, 0)	441	441	697,296	(5, 3, 0)	1	15	60
(2, 0, 0)	1	1	1	(5, 3, 1)	19	505	5620
(2, 0, 1)	1	1	1	(5, 3, 2)	278	9250	302,060
(2, 0, 2)	3	3	9	(5, 5, 0)	10	297	6984
(2, 0, 3)	8	10	83	(5, 5, 1)	329	12,905	892,640
(2, 0, 4)	30	39	1023	(5, 7, 0)	114	4725	688,080
(2, 2, 0)	2	2	5	(6, 0, 0)	0	0	0
(2, 2, 1)	12	16	107	(6, 0, 1)	0	0	0
(2, 2, 2)	72	105	2128	(6, 0, 2)	1	10	20
(2, 2, 3)	431	689	44,392	(6, 0, 3)	4	145	760
(2, 4, 0)	9	10	138	(6, 2, 0)	0	0	0
(2, 4, 1)	111	170	7206	(6, 2, 1)	2	105	420
(2, 4, 2)	1229	2004	279,348	(6, 2, 2)	31	2615	28,820
(2, 6, 0)	49	66	5606	(6, 4, 0)	2	105	840
(2, 6, 1)	1112	1833	526,228	(6, 4, 1)	47	5835	134,640
(2, 8, 0)	338	511	293,080	(6, 6, 0)	21	2865	138,000
(3, 1, 0)	1	1	1	(7, 1, 0)	0	0	0
(3, 1, 1)	3	7	17	(7, 1, 1)	0	0	0
(3, 1, 2)	15	42	291	(7, 1, 2)	2	280	1120
(3, 1, 3)	78	255	5293	(7, 3, 0)	0	0	0
(3, 1, 4)	438	1592	105,069	(7, 3, 1)	4	1260	10,080
(3, 3, 0)	3	7	38	(7, 5, 0)	2	945	15,120

where E_n is the identity group of permutations on n objects. A relation between the connected and total counting series also exists in this situation [13]; the explicit formula is

$$\prod_{\text{unlabelled}} (1 - x_1^{n_1} x_3^{n_3} x_4^{n_4})^{-p_1^{n_1 n_3 n_4}} \cdot \prod_{\text{labelled}} \exp\left(\frac{p_1^{n_1 n_3 n_4}}{n_1!} x_1^{n_1} x_3^{n_3} x_4^{n_4}\right) = 1 + \sum_{\substack{n_1, n_3, n_4 = 0 \\ n_1 + n_3 + n_4 > 0}}^{\infty} \frac{P_1^{n_1 n_3 n_4}}{n_1!} x_1^{n_1} x_3^{n_3} x_4^{n_4}, \tag{4}$$

which combines is an elegant way the formulas valid either when all nodes are labelled or when all nodes are unlabelled. The product called *labelled* is over all indices that produce a labelled graph (that is, $n_1 \neq 0$) while in the other product all indices for which no labelled nodes appear must be considered ($n_1 = 0$). This relation enabled us to compute the numbers $p_1^{n_1 n_3 n_4}$, also listed in Table I. Some of these values (the ones that enumerate trees) may be cross-checked at once: as it is well known, the number of trees with partition $(n_1 = n_3 + 2n_4 + 2, n_3, n_4)$ and of all nodes labelled is given by

$$T_L^{n_3 n_4} = \frac{(2n_3 + 3n_4)!}{2!^{n_3}\, 3!^{n_4}}. \tag{5}$$

If only the endnodes are labelled, the number is instead

$$T_1^{n_3 n_4} = \frac{T_L^{n_3 n_4}}{n_3!\, n_4!}. \tag{6}$$

This is a consequence of the fact that $\Gamma_I(G)$ reduces to the identity group when G is a tree.

The previous tests cover steps (1) and (2). For the last step some more refined tests are indispensable. A few chosen lagrangians will now be considered, and in each case the number of diagrams (and/or a related quantity, to be explained in the following) for various physical processes will be given. These results should then be reproduced by an operational computer program.

Itzykson and Zuber [14] have developed a technique to enumerate Feynman diagrams, based on a reduction to a zero-dimensional field theory (see also Ref. [15]), which I have adopted. The correlation functions of the zero-dimensional field theory are power series (with rational coefficients) of the coupling constant g; the coefficient of the monomial in g^m is sum of the (topological) symmetry factors of all Feynman diagrams of order m contributing to that correlation function. Only for situations where symmetry is absent (I mean when the symmetry factor is always 1, as in QED) does one obtain the real number of diagrams. We will call this weighted enumeration. It should be clear that, unless otherwise stated, all unrenormalized diagrams (including tadpoles, for example) are counted and generated.

As a first example let us consider a single self-conjugate field a with cubic and quartic interaction terms. The zero-dimensional theory reads

$$S_1 = -\frac{1}{2} a^2 + \frac{g}{6} a^3 + \frac{g^2}{24} a^4. \tag{7}$$

The first few terms of chosen correlation functions have been computed. The real number of diagrams may be

computed directly from Table I; the ρ-loop n_1-point function has

$$\sum_{n_4=0}^{[k/2]} p_1^{n_1, k-2n_4, n_4} \tag{8}$$

diagrams, where $k = n_1 - 2 + 2\rho$. Both results are listed in Appendix A.

As an illustration consider the two-loop tadpole diagrams, drawn in Fig. 2. These are diagrams of order g^3, so their number is $p_1^{130} + p_1^{111} = 3 + 3$ and the sum of the symmetry factors is $\frac{31}{24}$ according to (A4) and (A5). The symmetry numbers have been decomposed into a product of a local and a global piece, as discussed in the previous section.

One could also consider scalar theories with a single interaction term, either cubic or quartic. Although this has been done the complete results are not presented since in those cases one has nothing but a subset of the diagrams of the theory with both couplings. However, it should be clear that for those theories one may also compute the real number of diagrams from Table I.

A somewhat more complex case is given by the action

$$S_2 = -a\bar{a} + \frac{g}{6}(a^3 + 3a^2\bar{a} + 3a\bar{a}^2 + \bar{a}^3) + \frac{g^2}{24}(a^4 + 4a^3\bar{a} + 6a^2\bar{a}^2 + 4a\bar{a}^3 + \bar{a}^4). \tag{9}$$

It describes a "charged" field a with all possible cubic and quartic self-interaction terms. We shall not be concerned about "charge" nonconservation nor about other conservation laws; the only aim is to find diagrams that satisfy certain matching rules. This situation is already complex from the field theory point of view (there are nine types of vertices), although there is only one field. However, from the mathematical point of view, it is quite simple: the Feynman graphs are all the digraphs that may be drawn with the usual valency and labelling constraints. It will be shown below how to enumerate the Feynman diagrams in this theory.

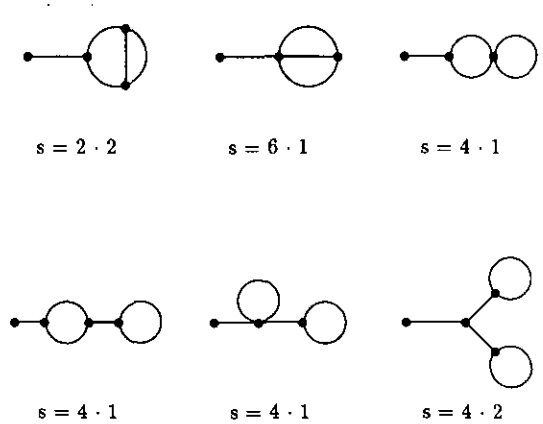

FIG. 2. Connected two-loop tadpole diagrams in the scalar theory S_1. Symmetry numbers are given as a product of a local (left) and a global part (right), as defined in the text. The number of diagrams is $p_1^{130} + p_1^{111} = 6$ and the sum of the symmetry factors is $\frac{31}{24}$, according to (A4) and (A5). Only the diagrams in the top row are 1P-I and the sum of the symmetry factors is $\frac{2}{3}$ as given in (B22).

Let $D_1^{n_1 n_3 n_4}$ be the number of possibly disconnected digraphs with labelled endnodes; they may be evaluated as [11]

$$D_1^{n_1 n_3 n_4} = N\{Z(E_{n_1}[S_1] \times S_{n_3}[S_3] \times S_{n_4}[S_4]) * Z(S_l[E_2])\}. \tag{10}$$

It has been described above how to compute the number of connected digraphs of this type $d_1^{n_1 n_3 n_4}$ (see Eq. (4)). These numbers are not the ones given by the diagram generator since not all constraints have been taken into account. The number $d_1^{n_1 n_3 n_4}$ may be obtained by adding together the number of diagrams contributing to all $n_1 + 1$ Green functions $\langle a^k \bar{a}^{n_1 - k} \rangle$ with n_1 legs and including, for each of these functions, a factor $n_1!/(n_1 - k)!/k!$ to account for all the different ways of labelling the legs.

An additional symmetry will simplify things. In the first place one may note immediately that Green functions differing only by the labelling of their legs must have the same number of diagrams. Now consider the two sets of Feynman graphs obtained from the Green functions $\langle a^k \bar{a}^{n_1 - k} \rangle$ and $\langle a^m \bar{a}^{n_1 - m} \rangle$ after selecting only the ones with n_3 cubic interactions and n_4 quartic interactions. If one takes the first set of diagrams and, in a systematic way, one replaces $k - m$ legs of type a (assume $k > m$) by $k - m$ legs of type $\bar{a}$ (this is possible since all interaction vertices exist), one will obtain the other set of diagrams; and since the legs are labelled, this procedure is one-to-one. It has been shown that all the 2^{n_1} possibilities considered above lead to the same number of digraphs and thus the expected number of Feynman diagrams with n_1 legs, n_3 cubic vertices, and n_4 quartic vertices is

$$\bar{d}_1^{n_1 n_3 n_4} = \frac{1}{2^{n_1}} d_1^{n_1 n_3 n_4}. \tag{11}$$

The only exception occurs when the diagrams have no interaction vertices, that is, for the tree level 2-point correlation functions, since only $\langle a\bar{a} \rangle$ is non-vanishing. In that case one has

$$\bar{d}_1^{200} = \tfrac{1}{2} d_1^{200}. \tag{12}$$

An equation similar to (8) also holds here, and in this way one obtains the counting series equations (A8).

The simpler action

$$S_2' = -a\bar{a} + \frac{g}{6}(a^3 + \bar{a}^3) + \frac{g^2}{24}(a^4 + \bar{a}^4) \qquad (13)$$

gives Feynman diagrams in a one to one correspondence with bichromatic graphs. Again, these diagrams are a subset of those for S_2 and so no numerical evaluation has been attempted.

The next situation involves three neutral scalars with a single cubic interaction

$$S_3 = -\tfrac{1}{2}a^2 - \tfrac{1}{2}b^2 - \tfrac{1}{2}c^2 + gabc. \qquad (14)$$

Here the Feynman graphs are graphs with labelled endnodes whose edges are coloured with three colours in such a way that at each interaction node all adjacent lines have different colours. This example will test the colouring algorithm ability to deal with different particles.

The last example, a scalar QED type theory, combines all features discussed above: different particles, several types of couplings, directed and undirected propagators. The action reads

$$S_4 = -\frac{1}{2}a^2 - b\bar{b} + gab\bar{b} + \frac{g^2}{2}a^2b\bar{b} + \frac{g^2}{4}b^2\bar{b}^2. \qquad (15)$$

It may be noticed that in all the examples presented cubic vertices have strength g and quartic vertices strength g^2. In this way all counting series obtained, which are power series in the coupling constant, will be in agreement with the loop expansion.

Other examples could be easily imagined, but I believe the ones just presented already provide a serious check for any computer program whose algorithm is interaction independent. The tests cover all possible features: connectedness, node labelling, edge directing, and edge colouring. For very complex situations like the standard model or the minimal supersymmetric model a computation of this type would be prohibitive. In those cases it can be argued that: steps 1 and 2 are the same whatever the lagrangian, and they have passed several stringent tests; no type of interaction is singled out by the colouring algorithm, which has given the right answer for various types and numbers of vertices. For these reasons, this algorithm seems to provide a more systematic approach to the subject.

As previous authors have devoted their attention to QED, I have also dealt with that case (which is a special case of scalar QED in the sense that the diagrams involved are a subset of those for scalar QED). Subroutines for the elimination of 1P reducible graphs and graphs excluded by Furry's theorem have been developed. The well-known numbers for the irreducible vertex Γ, the vacuum polarization Π, and the electron self-energy Σ have been reproduced.

5. THE COMPUTER PROGRAM

In its present form, the computer program performs a combinatorial exercise only. It does not generate symbolic expressions for the amplitudes corresponding to the generated diagrams; neither is there a graphical output at the moment.

The program generates all Feynman diagrams contributing to a given process and for a chosen loop order. This implies that there can be no bilinear interaction terms in the tree level lagrangian (only the properly diagonalized mass eigenstates can be used). At present it is also required that the interaction terms are either cubic or quartic in the fields, which is satisfied by gauge field theories. There are also some restrictions on the number of external particles n_1 and the loop order ρ accepted as input. The following bounds are likely to cover most practical situations:

$$\begin{aligned} &1 \leqslant n_1 \leqslant 7 \\ &0 \leqslant \rho \leqslant 4 \\ &2 \leqslant n_1 + \rho \leqslant 7. \end{aligned} \qquad (16)$$

In principle it is possible to use larger values by increasing array dimensions and updating a few parameters; in practice, if ever needed, it might take too long to run. Just remember that the number of diagrams usually grows in a faster than exponential way with both ρ and n_1. The feasibility of this algorithm also depends on the fact that the

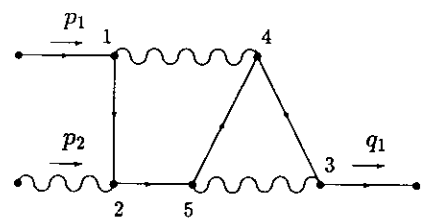


```
[#2,s=1]
[e-,p1,1]   [A,p2,2]   [e-,q1,3]   [e-,1,2]
[A,1,4]     [e-,2,5]   [e-,4,3]     [A,3,5]
[e-,5,4]
```

FIG. 3. Example of a Feynman diagram in QED contributing to the electron anomalous magnetic moment, and the way it is written on the output file. External particles are given a label p_i (incoming) or q_j (outgoing). An auxiliary numbering of the interaction vertices is used. For example, $[e-, 4, 3]$ means that there is an electron propagator directed from vertex 4 to vertex 3, and $[A, p2, 2]$ stands for an incoming photon with "4-momentum" p_2 that flows into vertex 2. The first line contains the number of the diagram as generated by the program (left) and its symmetry number (right).

TABLE II

Execution Time on a VAX-8550 for Processes in the Scalar Theory S_1

Green's function	Loop order	N	t (s)	N_I	t_I (s)
$\langle a \rangle$	4	471	2		
$\langle a^2 \rangle$	4	5076	47	1011	8
$\langle a^3 \rangle$	3	3729	4	619	2
$\langle a^3 \rangle$	4	70,600	349	11,388	62
$\langle a^4 \rangle$	2	2214	2		
$\langle a^4 \rangle$	3	50,051	45	6166	12
$\langle a^5 \rangle$	2	28,365	17	2230	3
$\langle a^6 \rangle$	1	11,460	9	390	1
$\langle a^7 \rangle$	0	2485	5		

Note. Values less than 1 s have been omitted. N is the number of the unrenormalized diagrams and N_I is the number of one-particle irreducible diagrams; t and t_I denote execution time (in seconds). The values N_I have not been computed theoretically, unlike the weighted values in (B22).

order of Γ_P is fairly small for connected graphs ($|\Gamma_P| \leqslant 72$ if inequalities (16) are satisfied), so that the full point symmetry group may be easily stored in the memory.

Two input files are used; one contains a simplified version of the lagrangian (only the combinatorial part) and the other describes the process, the loop order, and a few options, like the elimination of diagrams with tadpole insertions or one-particle reducible graphs. There is also an option that will list all Feynman graphs in a codified form. An example is given in Fig. 3.

To have an idea of the computer program performance (in its present form), Table II lists the CPU-time (on a VAX-8550) needed to generate the diagrams in the scalar theory S_1. Values listed include the computation of the symmetry factors and some internal checks. Values omitted are less than 1 s. I expect that a refined algorithm may improve the CPU-time required for pseudograph generation.

For theories with a larger number of vertices the number of diagrams may be much larger than in theory S_1 and typically one must add 10^{-4} to 10^{-3} s per diagram to the CPU-time just quoted. For example, the generation of all 32,726,641 distinct Feynman diagrams for the four-loop three-point function in theory S_2 takes a little over 2.5 h. As an example of a situation more close to reality, take the process $e^+e^- \to W^+W^-$ in the standard model at one loop. With 154 interaction vertices (all Higgs couplings were retained but gluons were discarded and quarks were colourless) in the Feynman–'t Hooft gauge, 2672 diagrams were generated in 0.9 s.

6. CONCLUDING REMARKS

A general algorithm for automatic Feynman graph generation has been described; this was implemented in a FORTRAN computer program. A simplified flow chart is shown in Fig. 4. The elimination of equivalent diagrams is complete. The algorithm works at its best when there are many Feynman graphs with the same underlying topology; this will be the case in higher loop expansion in usual gauge field theories (e.g., the standard model or its minimal supersymmetric extension).

Another advantage of this method is the following: the computer program requires constant (≈ 100 Kbytes) working space, regardless of the number of diagrams involved. This is because the algorithm was specifically designed to generate a single graph per step, and the elimination procedures can apply without reference to previously generated graphs. Moreover, the algorithm is not recursive (that is, it does not generate larger diagrams from a list of smaller diagrams). Thus no large diagram storage is necessary for generation purposes.

This algorithm generates all unrenormalized diagrams. After a renormalization procedure is applied to a given field

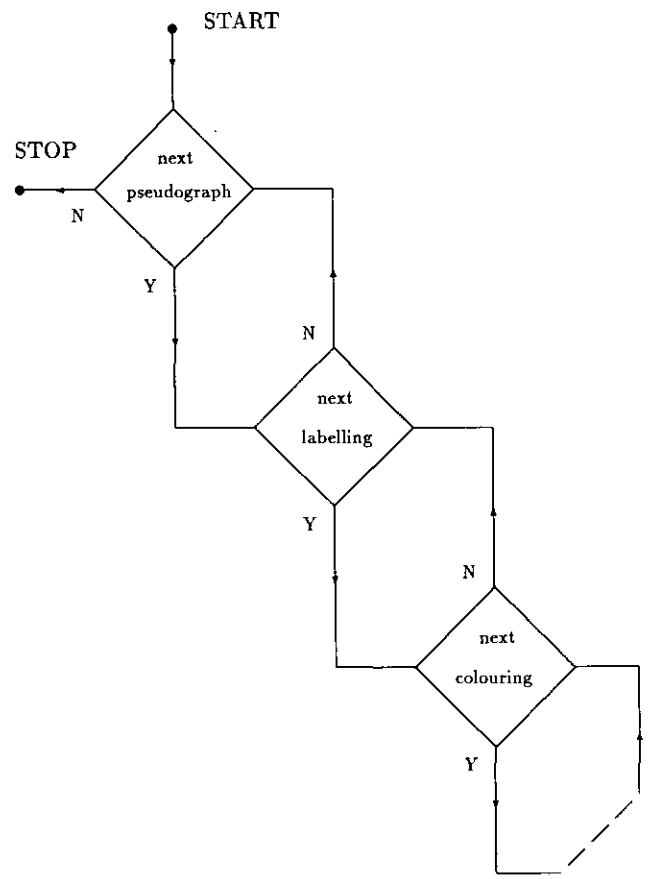

FIG. 4. Simplified algorithm flow chart showing a fully nested architecture. In each module **next structure** the program looks for a representative structure that has not been generated before (no comparison with previously generated structures is done, though). The inner loop, more precisely the dashed line, is the place where the Feynman diagrams may be counted and displayed (among other things).

theory, certain classes of diagrams are no longer considered. This requires that supplementary elimination routines must be written (in fact, a few of them are available); on the other hand, the algorithm can be easily adapted to different renormalization schemes. A copy of this program is available on request.

APPENDIX A: COUNTING SERIES OF SELECTED CORRELATION FUNCTIONS

In Section 4 the problem of testing an automatic Feynman diagram generator was addressed. Several chosen field theories were considered, and in each case the (weighted and/or exact) number of diagrams of selected correlation functions has been computed for low orders of perturbation theory. In this appendix are listed the first few terms of those counting series.

Let $G(X)$ be the connected correlation function $\langle X\rangle$ given by the zero-dimensional method [14], whose coefficients give the sum of the Feynman diagram symmetry factors. In turn, $N(X)$ stands for the counting series of the same correlation function, obtained from combinatorial graph theory methods [11]. All the numbers listed below, whose computation relies on theoretical methods, have been reproduced by the computer program. In all cases only connected diagrams were considered.

The technique used to compute the correlation functions is as follows [14] (consider, for instance, the theory S_1). Start with the functional generator

$$Z(J)=\int \frac{da}{\sqrt{2\pi}}\exp(S_1+Ja) \tag{A1}$$

and compute the complete Green's functions by expanding in the interaction terms up to a desired order

$$z_n=\left.\frac{\partial^n Z}{\partial J^n}\right|_{J=0}=\sum_{k,m=0}^{\infty}\frac{1}{k!\,m!}\left(\frac{g}{6}\right)^k\left(\frac{g^2}{24}\right)^m \times\int\frac{da}{\sqrt{2\pi}}a^{n+3k+4m}e^{-a^2/2}. \tag{A2}$$

Then the connected Green's functions may be obtained from

$$G(a^n)=\left.\left(\frac{\partial^n \log Z}{\partial J^n}\right)\right|_{J=0}. \tag{A3}$$

This gives

$$\begin{aligned}
G(a)&=\tfrac{1}{2}g+\tfrac{31}{24}g^3+\tfrac{341}{48}g^5+\tfrac{22,949}{384}g^7+\cdots\\
G(a^2)&=1+\tfrac{3}{2}g^2+\tfrac{25}{3}g^4+\tfrac{1741}{24}g^6+\tfrac{80,299}{96}g^8+\cdots\\
G(a^3)&=g+\tfrac{15}{2}g^3+\tfrac{1777}{24}g^5+\tfrac{44,177}{48}g^7+\tfrac{5,292,685}{384}g^9+\cdots\\
G(a^4)&=4g^2+57g^4+\tfrac{5,057}{6}g^6+\tfrac{167,621}{12}g^8+\cdots\\
G(a^5)&=25g^3+\tfrac{1149}{2}g^5+\tfrac{280,735}{24}g^7+\cdots\\
G(a^6)&=220g^4+7230g^6+\cdots\\
G(a^7)&=2485g^5+\cdots
\end{aligned} \tag{A4}$$

while for the exact enumeration (see (8) and Table I) one obtains

$$\begin{aligned}
N(a)&=g+6g^3+46g^5+471g^7+\cdots\\
N(a^2)&=1+3g^2+29g^4+351g^6+5076g^8+\cdots\\
N(a^3)&=g+14g^3+217g^5+3729g^7+70,600g^9+\cdots\\
N(a^4)&=4g^2+99g^4+2214g^6+50,051g^8+\cdots\\
N(a^5)&=25g^3+947g^5+28,365g^7+\cdots\\
N(a^6)&=220g^4+11,460g^6+\cdots\\
N(a^7)&=2485g^5+\cdots.
\end{aligned} \tag{A5}$$

The action S_2 has an intrinsic symmetry that may be used to relate correlation functions with the same number of legs:

$$G(a^r\bar{a}^s)=G(a^{r+s})+\delta_{1,r}\delta_{1,s}. \tag{A6}$$

Therefore it is sufficient to list the correlation functions of the form $\langle a^n\rangle$:

$$\begin{aligned}
G(a)&=g+\tfrac{46}{3}g^3+\tfrac{1592}{3}g^5+\tfrac{253,552}{9}g^7+\cdots\\
G(a^2)&=5g^2+178g^4+\tfrac{29,416}{3}g^6+\tfrac{6,427,984}{9}g^8+\cdots\\
G(a^3)&=g+46g^3+\tfrac{8612}{3}g^5+\tfrac{676,960}{3}g^7+\tfrac{192,148,160}{9}g^9+\cdots\\
G(a^4)&=7g^2+634g^4+59,348g^6+\tfrac{18,657,056}{3}g^8+\cdots\\
G(a^5)&=80g^3+11,624g^5+\tfrac{4,491,520}{3}g^7+\cdots\\
G(a^6)&=1280g^4+266,120g^6+\cdots\\
G(a^7)&=26,320g^5+\cdots.
\end{aligned} \tag{A7}$$

From Table I one obtains

$$\begin{aligned}
N(a)&=g+25g^3+880g^5+48,116g^7+\cdots\\
N(a^2)&=6g^2+254g^4+15,023g^6+1,144,071g^8+\cdots\\
N(a^3)&=g+55g^3+3875g^5+328,717g^7\\
&\quad+32,726,641g^9+\cdots\\
N(a^4)&=7g^2+741g^4+77,405g^6+8,745,435g^8+\cdots\\
N(a^5)&=80g^3+13,364g^5+1,905,400g^7+\cdots\\
N(a^6)&=1280g^4+302,220g^6+\cdots\\
N(a^7)&=26,320g^5+\cdots.
\end{aligned} \tag{A8}$$

Next follow the expansions in theory S_3, where weighted and exact enumerations coincide. The list includes only non-vanishing and symmetry unrelated counting series:

$$\begin{aligned}
G(a^2) &= 1 + g^2 + 4g^4 + 25g^6 + 208g^8 + \cdots \\
G(abc) &= g + 4g^3 + 25g^5 + 208g^7 + 2146g^9 + \cdots \\
G(a^2b^2) &= 2g^2 + 16g^4 + 150g^6 + 1664g^8 + \cdots \\
G(a^4) &= 6g^4 + 84g^6 + 1116g^8 + \cdots \\
G(a^3bc) &= 6g^3 + 84g^5 + 1116g^7 + \cdots \\
G(a^2b^2c^2) &= 32g^4 + 636g^6 + \cdots \\
G(a^4b^2) &= 24g^4 + 504g^6 + \cdots \\
G(a^6) &= 120g^6 + \cdots \\
G(a^3b^3c) &= 180g^5 + \cdots \\
G(a^5bc) &= 120g^5 + \cdots .
\end{aligned} \tag{A9}$$

The final listing is for the scalar QED type theory, for which the exact enumeration is missing:

$$\begin{aligned}
G(a) &= g + \tfrac{11}{2}g^3 + \tfrac{241}{4}g^5 + \tfrac{7757}{8}g^7 + \cdots \\
G(a^2) &= 1 + 2g^2 + \tfrac{47}{2}g^4 + \tfrac{837}{2}g^6 + \tfrac{75,043}{8}g^8 + \cdots \\
G(b\bar{b}) &= 1 + \tfrac{7}{2}g^2 + \tfrac{149}{4}g^4 + \tfrac{4789}{8}g^6 + \tfrac{199,199}{16}g^8 + \cdots \\
G(a^3) &= 5g^3 + 129g^5 + \tfrac{13,851}{4}g^7 + \tfrac{413,465}{4}g^9 + \cdots \\
G(ab\bar{b}) &= g + 14g^3 + \tfrac{1017}{4}g^5 + \tfrac{22,915}{4}g^7 + \tfrac{2,450,261}{16}g^9 + \cdots \\
G(a^4) &= 21g^4 + 888g^6 + \tfrac{133,371}{4}g^8 + \cdots \\
G(a^2b\bar{b}) &= 3g^2 + 77g^4 + \tfrac{8345}{4}g^6 + \tfrac{250,599}{4}g^8 + \cdots \\
G(b^2\bar{b}^2) &= 3g^2 + \tfrac{167}{2}g^4 + \tfrac{9155}{4}g^6 + \tfrac{136,851}{2}g^8 + \cdots \\
G(a^5) &= 114g^5 + 7305g^7 + \cdots \\
G(a^3b\bar{b}) &= 12g^5 + 525g^5 + 19,956g^7 + \cdots \\
G(ab^2\bar{b}^2) &= 16g^3 + 675g^5 + \tfrac{49,533}{2}g^7 + \cdots \\
G(a^6) &= 780g^6 + \cdots \\
G(a^4b\bar{b}) &= 66g^4 + 4305g^6 + \cdots \\
G(a^2b^2\bar{b}^2) &= 108g^4 + 6392g^6 + \cdots \\
G(b^3\bar{b}^3) &= 99g^4 + \tfrac{12,225}{2}g^6 + \cdots \\
G(a^5b\bar{b}) &= 450g^5 + \cdots \\
G(a^3b^2\bar{b}^2) &= 876g^5 + \cdots \\
G(ab^3\bar{b}^3) &= 927g^5 + \cdots .
\end{aligned} \tag{A10}$$

APPENDIX B: THE ENUMERATION OF SPECIAL TYPES OF DIAGRAMS

One-particle irreducible (1P-I) diagrams are the ones that do not become disconnected by cutting a single internal line. Since this characterization is purely topological, it may be done during step 1 of the program. This also means it is enough to consider the scalar theory of a single self-interacting self-conjugate field to do a complete test of the algorithm that identifies 1P-I graphs.

By using the Dyson–Schwinger equations, Cvitanović *et al.* [15] have developed a technique that produces differential equations to be satisfied by the various n-point functions (also for 1P-I functions). Nevertheless I have used another technique, more suitable for automated computation; the (algebraic) equations so obtained are valid for a whole class of models (they are satisfied for any number of self-interaction terms of the scalar field). This method is not very efficient for very high orders of perturbation theory, neither it is suited for asymptotic analysis, but it is very easy to implement and it works fairly well for small orders (say, up to g^{15}), which is the case of interest here.

Consider the functional generators W and Γ, of connected and 1P-I Green functions,

$$\begin{aligned}
W(J) &= \sum_{n=0}^{\infty} \frac{w_n}{n!} J^n \\
\Gamma(\Phi) &= \sum_{m=0}^{\infty} \frac{\gamma_m}{m!} \Phi^m
\end{aligned} \tag{B11}$$

which are related by a Legendre transformation [16]

$$\Gamma(\Phi) = W(J) - J\Phi, \qquad J = -\frac{\partial \Gamma}{\partial \Phi}, \qquad \Phi = \frac{\partial W}{\partial J}. \tag{B12}$$

A direct substitution leads to

$$\Gamma(\Phi) = \sum_{m=0}^{\infty} \frac{w_m}{m!} \left(-\frac{\partial \Gamma}{\partial \Phi} \right)^m + \Phi \frac{\partial \Gamma}{\partial \Phi}. \tag{B13}$$

This nonlinear equation can be given a formal solution. Since, due the super-exponential growth of the coefficients, we are dealing with formal series anyway, this *must be* the real solution. Let

$$\mu_m = \sum_{i=0}^{\infty} w_{m+i} \frac{(-\gamma_1)^i}{i!} \tag{B14}$$

and assume for the moment that the 1P-I tadpole γ_1 is known. Then the 1P-I functions γ_m may be computed as

$$\begin{aligned}
\gamma_0 &= \mu_0 \\
\gamma_2 &= -1/\mu_2
\end{aligned} \tag{B15}$$

and, for $m \geqslant 1$,

$$\gamma_{m+2} = \mu_2^{-2m-1} \sum_{(j)} \times \frac{(-1)^{s-m-1}\, s!\, \mu_2^{2m-s} \mu_3^{j_1} \mu_4^{j_2} \cdots \mu_{m+2}^{j_m}}{j_1!\, 2!^{j_1} j_2!\, 3!^{j_2} \cdots j_m!\, (m+1)!^{j_m}}. \quad \text{(B16)}$$

The summation extends over all partitions of $m = j_1 + 2j_2 + \cdots + mj_m$ and for each partition we define $s = 2j_1 + 3j_2 + \cdots + (m+1)j_m$.

The 1P-I tadpole γ_1 is obtained by solving the equation

$$\mu_1 \equiv w_1 - w_2\gamma_1 + \frac{w_3}{2!}\gamma_1^2 - \cdots = 0, \quad \text{(B17)}$$

which can be done in two ways. The first one is to expand γ_1 in powers of g and solving iteratively for the coefficients. This gives a unique solution since $w_2 \neq 0$ when $g = 0$. The second process is to expand in powers of w_1/w_2; writing γ_1 as

$$\gamma_1 = \sum_{k=1}^{\infty} \frac{a_k}{k!} \eta_1^k \quad \text{(B18)}$$

where $\eta_m = w_m/w_2$ one obtains $a_1 = 1$ and

$$a_{k+1} = \sum_{(j)} \frac{(-1)^s\, s!\, \eta_3^{j_1} \eta_4^{j_2} \cdots \eta_{k+2}^{j_k}}{j_1!\, 2!^{j_1} j_2!\, 3!^{j_2} \cdots j_k!\, (k+1)!^{j_k}} \quad \text{(B19)}$$

for $k \geqslant 1$; the summation extends over all partitions of k and s is defined as before. Note the similarity with (B16).

Here are some explicit relations determined by (B16)

$$\gamma_3 = \frac{\mu_3}{\mu_2^3}$$

$$\gamma_4 = \frac{\mu_2\mu_4 - 3\mu_3^2}{\mu_2^5} \quad \text{(B20)}$$

$$\gamma_5 = \frac{\mu_2^2\mu_5 - 10\mu_2\mu_3\mu_4 + 15\mu_3^3}{\mu_2^7}$$

and (B19)

$$\begin{aligned} a_2 &= \eta_3 \\ a_3 &= -\eta_4 + 3\eta_3^2 \\ a_4 &= \eta_5 - 10\eta_3\eta_4 + 15\eta_3^3 \\ a_5 &= -\eta_6 + 15\eta_3\eta_5 + 10\eta_4^2 - 105\eta_4\eta_3^2 + 105\eta_3^4. \end{aligned} \quad \text{(B21)}$$

This procedure leads to the following 1P-I correlation functions (in theory S_1):

$$\begin{aligned} \gamma_1 &= \tfrac{1}{2}g + \tfrac{2}{3}g^3 + \tfrac{25}{8}g^5 + \tfrac{76}{3}g^7 + \cdots \\ \gamma_2 &= -1 + g^2 + \tfrac{41}{12}g^4 + \tfrac{55}{2}g^6 + \tfrac{15{,}275}{48}g^8 + \cdots \\ \gamma_3 &= g + \tfrac{5}{2}g^3 + \tfrac{89}{4}g^5 + \tfrac{2265}{8}g^7 + \tfrac{214{,}865}{48}g^9 + \cdots \\ \gamma_4 &= g^2 + \tfrac{21}{2}g^4 + \tfrac{709}{4}g^6 + \tfrac{26{,}625}{8}g^8 + \cdots \\ \gamma_5 &= 57g^5 + 1660g^7 + \cdots \\ \gamma_6 &= 390g^6 + \cdots \\ \gamma_7 &= 0g^5 + \cdots. \end{aligned} \quad \text{(B22)}$$

Next we return to the quantities μ_m defined in (B14). They enumerate diagrams without tadpole subdiagrams as it may be realized. A straightforward calculation gives

$$\begin{aligned} \mu_1 &= 0 \\ \mu_2 &= 1 + g^2 + \tfrac{53}{12}g^4 + \tfrac{106}{3}g^6 + \tfrac{28{,}523}{72}g^8 + \cdots \\ \mu_3 &= g + \tfrac{11}{2}g^3 + 46g^5 + 524g^7 + \tfrac{359{,}677}{48}g^9 + \cdots \\ \mu_4 &= 4g^2 + \tfrac{89}{2}g^4 + \tfrac{6797}{12}g^6 + \tfrac{206{,}015}{24}g^8 + \cdots \\ \mu_5 &= 25g^3 + \tfrac{929}{2}g^5 + \tfrac{32{,}985}{4}g^7 + \cdots \\ \mu_6 &= 220g^4 + \tfrac{11{,}975}{2}g^6 + \cdots \\ \mu_7 &= 2485g^5 + \cdots. \end{aligned} \quad \text{(B23)}$$

Let me point out that the power series expansions presented in this appendix (for example, the expansion of μ_m in powers of γ_1) are convergent in the sense that for computing the exact coefficients up to order g^m only a finite number of terms must be added. For instance, the first five terms in (B18) reproduce γ_1 up to g^9.

ACKNOWLEDGMENTS

I thank Professor R. C. Read for an enlightening discussion on graph enumeration and J. C. Romão for critical reading of the manuscript and useful comments. I also thank S. Eleutério for help in computer matters. In addition, I thank M. Perrottet for a discussion about FRENEY, and M. Dubinin for calling my attention to recent work in this area (which also includes the program GRACE [17], that generates tree-level and 1-loop diagrams).

REFERENCES

1. E. E. Boos *et al.*, Moscow State Univ., Institute for Nuclear Physics, Preprint 89-63/140.
2. J. A. Campbell and A. C. Hearn, *J. Comput. Phys.* **5**, 280 (1970).
3. M. Perrottet, in *Computing as a Language of Physics* (International Atomic Energy Agency, Vienna, 1972), p. 555; J. Calmet and M. Perrottet, *J. Comput. Phys.* **7**, 191 (1971).
4. T. Sasaki, *J. Comput. Phys.* **22**, 189 (1976).

5. T. Kaneko, S. Kawabata, and Y. Shimizu, *Comput. Phys. Commun.* **43**, 279 (1987).
6. J. Küblbeck, M. Böhm, and A. Denner, *Comput. Phys. Commun.* **60**, 165 (1990).
7. F. Harary, *Graph Theory* (Addison–Wesley, Reading, MA, 1969).
8. R. D. Cameron, C. J. Colbourn, R. C. Read, and N. C. Wormald, *J. Graph Theory* **9**, 551 (1985).
9. G. Sabidussi, *Am. J. Math.* **76**, 447 (1954).
10. A. C. Hearn, *REDUCE Users Manual, Version 3.2* (The Rand Corporation, 1985).
11. R. C. Read, *J. London Math. Soc.* **34**, 417 (1959).
12. R. J. Riddell and G. E. Uhlenbeck, *J. Chem. Phys.* **21**, 2056 (1953).
13. R. C. Read, private communication.
14. C. Itzykson and J. B. Zuber, *Quantum Field Theory* (McGraw–Hill, New York, 1980), p. 466.
15. P. Cvitanović, B. Lautrup, and R. B. Pearson, *Phys. Rev. D.* **18**, 1939 (1978).
16. G. Jona-Lasinio, *Nuovo Cimento* **34**, 1790 (1964)
17. T. Kaneko and H. Tanaka, University of Tokyo, Institute for Cosmic Ray Research, ICRR-Report-238-91-7.